Simulating thermal motion in crystalline phase-I ammonia

Article *in* The Journal of Chemical Physics · April 2010

DOI: 10.1063/1.3387952 · Source: PubMed

4 authors, including:

Carole A Morrison
The University of Edinburgh
170 PUBLICATIONS **3,796** CITATIONS

SEE PROFILE

Simulating thermal motion in crystalline phase-I ammonia

Anthony M. Reilly,[1] Scott Habershon,[2] Carole A. Morrison,[1,a)] and David W. H. Rankin[1]
[1]*School of Chemistry, University of Edinburgh, West Mains Road, Edinburgh EH9 3JJ, United Kingdom*
[2]*Department of Chemistry, Physical and Theoretical Chemistry Laboratory, University of Oxford, South Parks Road, Oxford OX1 3QZ, United Kingdom*

(Received 3 February 2010; accepted 22 March 2010; published online 6 April 2010)

Path-integral molecular dynamics have been used to simulate the phase-I crystalline form of ammonia, using an empirical force field. This method allows quantum-mechanical effects on the average geometry and vibrational quantities to be evaluated. When these are used to adjust the output of a high-temperature density functional theory simulation, the results are consistent with those given by the most recent structural refinement based on powder neutron diffraction data. It is clear that the original refinement overestimated thermal motion, and therefore also overestimated the equilibrium N–{H/D} bond length. © *2010 American Institute of Physics*. [doi:10.1063/1.3387952]

I. INTRODUCTION

The crystal structure of phase-I ammonia has been the focus of continued experimental and theoretical investigation for over 50 years. It has a cubic crystal structure in the $P2_13$ space group with four molecules in the unit cell, as shown in Fig. 1.[1] The interest in ammonia stems from its simple structure and its role as an archetypal example of a hydrogen-bonding network. It is also considered to be an important species in the study of the solar system,[2] with solid ammonia known to exist in the atmospheres of a number of the outer planets and their moons.[3,4]

In light of this, numerous experimental and theoretical investigations of the properties of phase-I ammonia have been performed. The deuterated crystal structure has been determined by powder neutron diffraction by Reed and Harris,[5] and more recently by Hewat and Riekel.[1] X-ray diffraction has also been employed,[6] as has diffuse neutron scattering.[7] Several groups have also studied the phonon spectrum of phase-I ammonia using infrared spectroscopy,[8,9] Raman spectroscopy,[8] and inelastic neutron scattering.[10] Simulations employing density functional theory (DFT)[11,12] or empirical models have also been employed.[13]

Given the numerous studies of phase-I ammonia in the literature, it is perhaps surprising that there is no definitive, accurate, and precise crystal structure available. Neutron diffraction is the method of choice for determining an accurate crystal structure of a system such as ammonia, with its light hydrogen atoms. However, the most recent neutron diffraction study of ammonia was performed by Hewat and Riekel in 1979.[1] They determined the crystal structure at 2, 77, and 180 K and applied librational corrections based on the translational, librational, and screw (TLS) tensor method[14] to the time-averaged experimental N–D bond length to determine an equilibrium value, free from the well known bond-shortening effects of librational motion.[15] Hewat and Riekel's data set was used in a later refinement by Leclercq *et al.*[16] using a special structure factor equation with the aim of determining an equilibrium geometry. However, the equilibrium structures and isotropic displacement parameters obtained by the two refinements differ significantly.

We have recently applied molecular dynamics (MD) simulations to the study of phase-I ammonia, with the aim of determining its equilibrium structure free from any approximations regarding thermal motion.[17] The MD simulations, performed at 77 K, gave much smaller estimates of thermal motion [in the form of anisotropic displacement parameters (ADPs)] and distance corrections than obtained in the original refinement of Hewat and Riekel. The agreement with the more recent refinement of Leclercq and co-workers was also far from sufficient to draw any meaningful conclusions.

In this paper, we expand on our previous investigations of the crystal structure of phase-I ammonia at 77 K by performing a classical Car–Parrinello MD simulation with a DFT force field at a higher temperature of 180 K. Our previous studies[11,12] of the phonon spectrum of phase-I ammonia showed that MD simulations using generalized-gradient approximation DFT functionals such as PBE (Ref. 18) and PW91 (Ref. 19 and 20) gave vibrational frequencies in good agreement with experimental values and higher-level hybrid-DFT lattice dynamics results. The MD-derived vibrational eigenvectors also permitted the reassignment of the symmetry of the experimentally observed frequencies. We may therefore expect DFT simulations to give a reasonable description of thermal motion in phase-I ammonia.

However, there are clearly a number of approximations and limitations inherent in the DFT simulations performed in this and previous studies. In particular, the computational expense of DFT limits these simulations to relatively small system sizes, and the use of classical MD to sample phase-space neglects the role of nuclear quantum effects in the thermal motion. Therefore, in order to assess the importance of finite-size effects and quantum-mechanical fluctuations, we have also performed both classical MD and quantum path integral MD (PIMD)[21,22] simulations using an empirical interaction potential. Performing simulations with two different descriptions of the interatomic interactions in the crystal enables us to assess the merits of the two refinements of the

a)Electronic mail: c.morrison@ed.ac.uk.

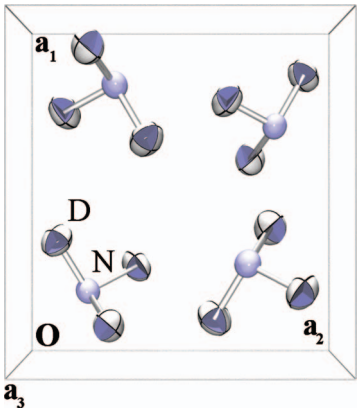

FIG. 1. Unit cell of phase-I ammonia (ND_3) with cubic ($P2_13$) space-group symmetry and a cell length of 5.185 Å; the labeled N and D atoms constitute the asymmetric unit. The thermal ellipsoids are plotted at the 50 % level using values from a 180 K DFT-MD simulation (see Sec. III A for more details).

crystal structure and to validate further our methodology for determining equilibrium structures from a combination of experimental and theoretical data. While our simulations have focused on ND_3 it is important to note that the equilibrium structures of ND_3 and NH_3 will be identical. The heavier mass of the D atom does affect the thermal motion of the system significantly but the equilibrium structure represents the system at rest with no thermal or zero-point motion.

The remainder of this paper is organized as follows. In Sec. II, we outline the computational approach taken in performing DFT MD simulations. We also give details of PIMD simulations employing an empirical force field. In Sec. III A, we describe the results of our DFT calculations, comparing the calculated thermal motion to that determined experimentally. In Sec. III B, we investigate the role of nuclear quantum effects in the thermal motion of phase-I ammonia.

II. SIMULATION METHODS

A. DFT simulation

A DFT MD simulation of phase-I deuteroammonia was carried out using a $2\times2\times2$ supercell with the CPMD program.[23] In total, this supercell contains 32 ammonia molecules. The PBE functional was used together with a plane-wave cut-off energy of 800 eV. This value converged the total energy and atomic forces to less than 1 meV $atom^{-1}$ and 1 meV $Å^{-1}$, respectively. Core-valence interactions were represented using the standard norm-conserving Martins–Troullier[24] psuedopotentials provided with the CPMD code. The electronic wave function was sampled at the Γ-point of the supercell, corresponding to a $2\times2\times2$ Monkhorst–Pack grid[25] of the unit cell. This degree of sampling was found to be sufficient in our previous studies of phase-I ammonia.[12,17]

The MD simulation was carried out at 180 K in the constant-*NVT* ensemble using the Car–Parrinello simulation method.[26] As in our previous DFT simulations at 77 K, the length of the unit cell was an optimized value of 5.185 Å; this choice clearly neglects thermal expansion of the crystal lattice, but facilitates comparison of the thermal motion at the two different temperatures. A massive Nosé–Hoover thermostat was used to regulate the temperature,[27] and a timestep of 0.09 fs was used to integrate the equations of motion. After 1.5 ps equilibration, configurations for later analysis were subsequently sampled every five steps during a 15 ps trajectory.

B. Empirical-potential simulations

To complement the DFT simulations, classical MD and quantum PIMD simulations of phase-I ammonia were carried out using a force field previously described by Hinchliffe *et al.*[13] Hinchliffe's model C (abbreviated to HC) comprises an electrostatic component, with a charge (+0.462 *e*) on each H/D atom and a charge (−1.386 *e*) on a site suspended below the N atom (toward the plane of the hydrogen atoms). The nonelectrostatic intermolecular interactions are split into dispersive components acting only between N atoms, repulsive interactions between all atoms and a mildly attractive interaction between N and H atoms. This force field was developed for rigid-body simulations so the harmonic bond stretches and angle bends suggested by Diraison *et al.*[28] were used to model the intramolecular degrees of freedom in our calculations.

Classical MD and PIMD[21,22] simulations were performed under constant-*NVT* conditions. In all simulations, a time-step of 0.5 fs was used. In the classical MD simulations, the equations of motion were integrated with the velocity-Verlet algorithm;[29] a symplectic integrator employing alternating external force and free ring-polymer evolution steps was employed in the PIMD simulations. Correct thermal sampling was achieved in each case using an Andersen thermostat.[30] Configurations were sampled every fifth time-step in a 20 ps simulation, following a 1.5 ps equilibration period.

Preliminary simulations suggested that the experimental cell parameters for phase-I ammonia were unsuitable for simulations with the HC empirical potential. Instead, finite-temperature cell vectors at 77 and 180 K were determined by performing a classical MD simulation using a $4\times4\times4$ supercell with Monte Carlo[29] relaxation of the cell vectors. Three simulations of 0.5 ns length with different initial cell parameters were performed at both temperatures. The three simulations gave finite-temperature cell parameters within 0.01 Å of each other, a sufficient precision for the purposes of the present study.

Two quantum PIMD simulations,[21,22] using $P=32$ and $P=64$ beads, were performed at 77 and 180 K. In each case, $4\times4\times4$ supercells with the classically determined finite-temperature cell lengths were used for the simulations at both temperatures. Although the cell vectors in the quantum simulations would be expected to be slightly different due to the effects of quantum fluctuations, our approach at least allows direct comparison of the results of the classical and quantum simulations.

In all calculations, electrostatic interactions were calculated using the standard Ewald summation technique.[29] The minimum-image convention was observed for the dispersion

forces with interactions being truncated at a distance of half the size of the supercell (~9.6 Å in the case of a $4\times4\times4$ supercell).

C. Trajectory analysis

Time-averaged atomic positions were calculated numerically from the simulation data using the full space-group and supercell symmetry. Here,

$$\mathbf{r}_a = (\overline{u_1}, \overline{u_2}, \overline{u_3}), \tag{1}$$

$$\overline{u_i} = \frac{1}{N\times S}\sum_{n=1}^{N}\sum_{j=1}^{S} u_{i,j,n} = \langle u_i \rangle, \tag{2}$$

where N is the total number of steps the average is calculated over, S is the total number of symmetry-related atoms in the supercell, and $u_{i,n}$ is the value of the ith component of the atomic position at step number n. There are 12 symmetry operations acting on the unit cell; the asymmetric unit consists of one deuterium atom and one third of a nitrogen atom. For path-integral simulations each of the P beads used to represent an atom was included in the averages such that $N\times S\times P$ data points were collected for the D atom. As the N atom lies on a threefold axis of symmetry, its three coordinates were averaged to obtain its single positional parameter.

The time-averaged theoretical position, $\mathbf{r}_{ave}^{MD}$, can be used in conjunction with the theoretical equilibrium (energy-minimized) position, $\mathbf{r}_e$, as corrections to an experimental structure, $\mathbf{r}_{ave}^{exp}$. Application of the corrections yields an experimental equilibrium structure, which we denote $\mathbf{r}_e^{MD}$, indicating that is obtained from MD-derived corrections. Specifically, these quantities are related according to

$$\mathbf{r}_e^{MD} = \mathbf{r}_{ave}^{exp} + (\mathbf{r}_e - \mathbf{r}_{ave}^{MD}) = \mathbf{r}_{ave}^{exp} + \Delta\mathbf{r}_{MD}. \tag{3}$$

This equation demonstrates how our simulation data regarding atomic thermal motion are used to correct the (time-averaged) experimental data in order to obtain an experimental equilibrium structure.

The standard thermal ellipsoids utilized to visualize most crystal structures represent surfaces of constant probability derived from the Gaussian probability density functions (PDFs), $P(\mathbf{r})$, that are used to model the thermal motion of each atom:

$$P(\mathbf{r}) = \frac{|\mathbf{U}^{-1}|^{1/2}}{(2\pi)^{3/2}}\exp\left(-\frac{1}{2}\mathbf{r}^T\mathbf{U}^{-1}\mathbf{r}\right), \tag{4}$$

where $\mathbf{U}$ is the covariance matrix of the atom of interest. This matrix has six unique elements, $U_{ij}(i,j=1,2,3)$, which are the ADPs commonly reported in crystal structure determinations. They can be estimated numerically from the simulation data using

$$U_{ij} = \langle (u_i - \overline{u_i})(u_j - \overline{u_j}) \rangle = \langle \Delta u_i \Delta u_j \rangle. \tag{5}$$

The U_{ii} values represent the variances or extent of the thermal motion, while the U_{ij} values give information on the orientation of the motion relative to the crystallographic axes.

Sampling errors in the mean and covariance matrix were estimated using the central limit theorem.[29] To remove the effect of correlations the blocking method[31] was applied to the DFT MD data. This had the effect of increasing the uncertainties by an order of magnitude. For the EP simulations, the large volume of data necessitated the calculation of Eqs. (2) and (5) "on the fly," which prevented the application of the blocking method. While the trajectory was sampled only every 10 steps to address this issue partially, the uncertainties in the case of the EP simulation remain very small, far smaller than the likely errors that arises from the use of empirical potentials.

As well as determining the standard mean and ADPs for comparison with experiment, the MD simulation can be used to determine the underlying PDFs numerically, free from any assumptions regarding a particular mathematical form. To this end, the positions adopted by an atom in the course of the simulation can be binned to form one-, two- (2D) or three-dimensional histograms, which yield the numerical PDF when normalized.

III. RESULTS AND DISCUSSION

A. DFT-MD simulation

Our previous study using simulations at 77 K found significant disagreement between the theoretical and experimental ADPs. Perhaps one of the most likely sources of error is the application of classical MD to model the motion of the nuclei. These classical calculations neglect the influence of zero-point-energy (ZPE) conservation and quantum-mechanical tunneling; both of these effects would be expected to play a significant role at the low temperatures investigated experimentally, particularly with regards to the motion of the light deuterium atoms.

However, fully converged PIMD simulations with a DFT force field are simply too expensive to perform in the present context. Instead, in order to investigate whether the discrepancies in our previous DFT simulations arose due to neglect of nuclear quantum effects, we performed DFT-MD simulations at the higher temperature of 180 K, where we might expect quantum fluctuations to be less important. Comparing the results of our simulations at two temperatures to the available experimental refinements then gives some indication of the reliability of our approach for extracting experimental equilibrium structures.

1. Experimental and simulated powder neutron diffraction structure at 180 K

The ADPs and bonded distance corrections determined in DFT MD simulations of phase-I ammonia at 180 K are presented in Table I; the previously reported values[17,32] at 77 K are provided for comparison, as are the earlier experimental (powder neutron diffraction) results of Hewat and Riekel. As expected, our results demonstrate large increases in the thermal motion as the temperature is increased; for example, the magnitudes of the calculated variances (U_{ii}) are seen to increase by around 50% in the two simulations. However, we find that our DFT simulation results are in disagreement with

TABLE I. Experimental (Ref. 1) and simulated (classical DFT MD) ADPs of the N and D atoms, together with the time-averaged bonded distance and equilibrium correction at 77 and 180 K. The experimental distance correction was derived using the TLS method. The MD correction is given by $\Delta r_{\mathrm{MD}}=r_{\mathrm{e}}-r_{\mathrm{ave}}^{\mathrm{MD}}$.

ADP ($\mathrm{Å}^2$)	77 K		180 K	
	DFT MD	Expt.	DFT MD	Expt.
N				
U_{ii}	0.0103(6)	0.0290(22)	0.0176(4)	0.0384(8)
U_{ij}	−0.0010(1)	−0.0015(15)	−0.0013(2)	−0.0014(5)
D				
U_{11}	0.0147(4)	0.0467(36)	0.0260(3)	0.0575(16)
U_{22}	0.0155(2)	0.0407(38)	0.0272(3)	0.0709(22)
U_{33}	0.0163(3)	0.0552(30)	0.0287(3)	0.0676(23)
U_{12}	−0.0038(1)	−0.0096(21)	−0.0066(1)	−0.0186(11)
U_{13}	0.0025(1)	0.0091(34)	0.0051(1)	0.0093(14)
U_{23}	−0.0004(1)	−0.0027(24)	−0.0005(1)	−0.0029(14)
$r(\mathrm{N-D})_{\mathrm{av}}$ (Å)	1.0281(36)	0.988(9)	1.0213(36)	0.989(5)
$\Delta r(\mathrm{N-D})$ (Å)	0.0083(36)	0.051(22)	0.0152(31)	0.069(9)

the refinement results of Hewat and Riekel. In most cases, our calculated ADPs are smaller than the experimentally derived values by around a factor of three.

Figure 1 shows the simulated thermal ellipsoids of the ammonia molecule. The thermal ellipsoids seem reasonable in size and orientation. The experimental ellipsoids determined by Hewat and Riekel are much larger and, at probability isosurfaces greater than 90%, begin to overlap. As well as plotting the harmonic PDFs, the numerical anharmonic PDFs can also be extracted from the MD simulation. The 2D PDFs of the D atom at 180 K are given in Fig. 2. It is relatively easy to orientate the numerical PDF along the harmonic principal axes of thermal motion. High-frequency noise distorts the raw numerical PDFs so a low-pass Fourier filter has been applied to the distributions plotted in Fig. 2 to aid visualization. In the case of the D atom the resulting PDFs do not appear to deviate that much from a Gaussian distribution, although there is a slight curvature visible in Fig. 2(a).

The TLS bond-distance corrections determined by Hewat and Riekel (Table I) are also very large and at 180 K the correction yields a librationally corrected bond length of 1.058 Å. The absolute value is significantly longer than the theoretical equilibrium value of 1.035 Å obtained previously using DFT calculations with the PBE and PW91 functional.[17] The TLS bond length is also much longer than the time-averaged interatomic N–D distance of 1.005(1) Å determined by Damay *et al.* using diffuse scattering.[7] No uncertainty was provided for the corrected bond length as the estimation of such quantities has only been made possible very recently.[33] However, the uncertainty will be probably be of the order of 0.005–0.010 Å (the time-averaged bond length uncertainty is 0.005 Å) and so the differences between the experimental values and DFT value are statistically significant. While Bragg scattering distances are affected by librational motion of the molecule, the distance obtained from diffuse scattering should be affected only by anharmonic vibrations of the two atoms relative to one another. For bonded atoms, such motion should be adequately modeled by a Morse oscillator. However, the time-averaged bond length of a Morse oscillator is always longer than the equilibrium distances as the potential is asymmetric, becoming shallower at longer distances. Thus the diffuse scattering distance should represent the upper limit of the equilibrium distance. A more detailed comparison with the 150 K diffuse scattering data is not possible as only the N–D and D···D interatomic distances were determined by the analysis employed. The nature of diffuse scattering means that atomic positions and estimates of the extent of individual atom's motions are not usually obtained.

The upshot of this comparison between DFT simulations and experiment is as follows. First, we find that our DFT simulations predict much smaller thermal motion for both N and D atoms than originally determined by experiment at both 77 and 180 K. Second, in our higher temperature simulations, we find that the agreement is no better between theory and experiment; as a result, these DFT simulations cannot be used to indicate whether nuclear quantum effects are important or not. Finally, we find that our DFT simulations result in much shorter equilibrium bond lengths than the experimental; encouragingly, our calculated bond length is closer to the experimental value determined by diffuse scattering, but is still too large.

2. Comparison to rerefined data set of Leclercq et al.

It is possible to shed some light on the results of our DFT simulations by comparing our results to a more recent

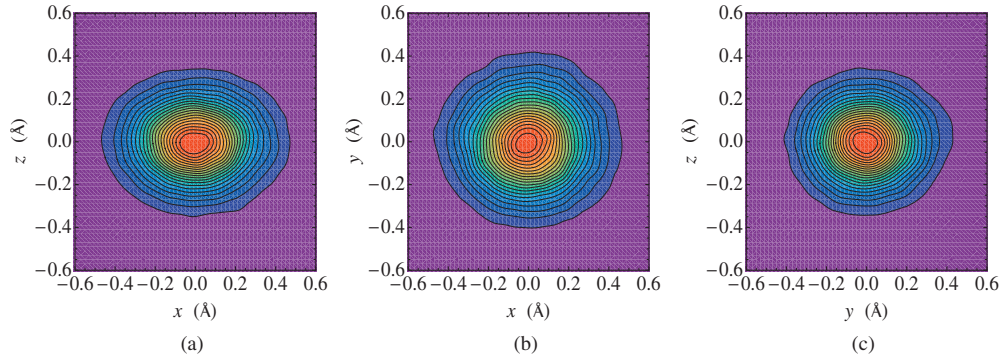

FIG. 2. Classical 2D probability distribution functions for the D atom in ND_3 at 180 K plotted in the (a) *xz*, (b) *xy*, and (c) *yz* planes. (*x* is the longest principal axis; *z* the shortest.)

TABLE II. Isotropic displacement parameters (U_{eq}) of the N and D atoms in ND_3 determined in classical DFT MD simulations. The results of refinements by Leclercq *et al.* (Ref. 16) and Hewat and Riekel (Ref. 1) are also shown.

T/K	Method	N ($Å^2$)	D ($Å^2$)
77	DFT MD	0.0103(6)	0.0155(3)
77	Leclercq *et al.*	0.0144(3)	0.0222(4)
77	Hewat and Riekel	0.0290(22)	0.0475(40)
180	DFT MD	0.0176(4)	0.0273(3)
180	Leclercq *et al.*	0.0166(4)	0.0243(5)
180	Hewat and Riekel	0.0384(8)	0.0653(24)

refinement of the Hewat and Riekel data. Here, Leclercq *et al.*[16] used a curvilinear structure factor equation which treated the D atoms as rotating around the C_3 axis of the ammonia molecule. As it was defined in an internal coordinate system of the molecule, this refinement yielded distances free from the effects of librational motion. Isotropic estimates of the amount of thermal motion of the atoms were also obtained. Table II gives the U_{eq} values as determined at 77 and 180 K from the $2\times2\times2$ supercell DFT MD simulations, as well as values determined in the two experimental refinements.

At the higher temperature of 180 K, the DFT MD results agree with the refinement of Leclercq *et al.* to within 3σ for the N atom and within 6σ for the D atom. This suggests that the original refinement of Hewat and Riekel was most likely flawed, possibly in its treatment of absorption. Leclercq *et al.* postulated that the difference between their refined values and those of Hewat and Riekel arose, in part, from the curvilinear nature of the structure factor, which in principle would neglect some of the librational contribution to the motion of the D atoms. However, this does not account for the differences in the N-atom values, and the close and relative agreement of the DFT values with those of Leclercq *et al.* suggests that the majority of the D-atom motion is correctly modeled by their structure factor.

With their curvilinear structure factor Leclercq *et al.* estimated an equilibrium N–D/H distance of 1.001(7) Å. Applying the 180 K MD distance correction of 0.0152 Å to the time-averaged distance of Hewat and Riekel yields an r_e^{MD} value of 1.004(6) Å. The agreement is encouraging but may well be fortuitous: it is clear that there are issues with the description of thermal motion in the original refinement and a new experimental time-averaged geometry must be determined to order to apply the MD method reliably. The geometry determined by Leclercq *et al.* neglects internal vibrations of the molecule, which may also affect the atomic positions and interatomic distances.

At the lower temperature of 77 K we find that the simulated values are in much better agreement with the refined values of Leclercq *et al.* than with the values of Hewat and Riekel. However, the differences are still relatively large compared to the experimental uncertainties; the simulated values are typically 15σ away from the refined values. Given that the agreement is much better at higher temperatures, this discrepancy is most likely to arise as a result of the neglect of quantum fluctuations such as ZPE and tunneling; we investigate these effects in Sec. III B 3 below.

3. Solid and gas-phase bond lengths

It is worth commenting here upon an apparent discrepancy in the calculated bond lengths of the ammonia molecule. The theoretical equilibrium N–D/H bond length in gas-phase ammonia is 1.0107 Å, determined using the coupled cluster method and extrapolation of large basis set results, while the experimental equilibrium value (calculated from microwave spectroscopic results with theoretical vibrational corrections) is 1.0114(6) Å.[34] Under the influence of hydrogen bonding, the N–D/H equilibrium bond length in the solid state would be expected to be longer than the gas-phase value but the solid-state bond length obtained from diffuse scattering measurements (1.005 Å), the equilibrium value of Leclercq *et al.* (1.001 Å), and the equilibrium value from the present work (1.004 Å) are all shorter than the gas-phase values. A DFT supercell calculation of an isolated ammonia molecule, using the same computational setup outlined in Sec. II together with a 15 Å cell size and a Poisson solver[35] to reduce electrostatic interactions between periodic images, gave a bond length of 1.029 Å, shorter than the DFT solid-state value of 1.035 Å. More precise solid-state structural studies would confirm whether the apparent experimental shortening of the bond upon condensation has any physical significance. A more recent single-crystal x-ray diffraction study of phase-I NH_3 was carried out by Boese *et al.*[6] The convolution of electron density and thermal motion means that a multipole refinement is required to achieve meaningful geometries with x-ray methods; however, while a multipole refinement was performed, the N–H bond was fixed at an empirical value of 1.01 Å.

B. Empirical-potential simulations

Further validation of the DFT results presented in the preceding section would require constant-*NPT* simulations, quantum PIMD simulations and the use of larger supercells. Simulations with a small number of path-integral beads are feasible, as might be simulations with a $3\times3\times3$ supercell. However, converging these results would not be possible with a DFT force field. To probe the importance of these factors we instead turn to empirical-potential simulations to provide further qualitative insight into the thermal motion of phase-I ammonia. In contrast to the DFT simulations, finite-temperature lattice vectors were used for these simulations. MC relaxation gave a value for the cell parameter of approximately 4.82 Å at 77 K, while at 180 K the lattice constant was roughly 4.89 Å. These values are approximately 5% smaller than the experimental values of 5.073 and 5.125 Å at 77 and 180 K, respectively, serving as an indication of the accuracy of the empirical force field.

1. System-size effects

Table III gives the isotropic displacement parameter for the N and D atoms determined for a variety of supercell sizes at a temperature of 77 K. The results suggest that quite large

TABLE III. Isotropic displacement parameters (U_{eq}) of the N and D atoms at 77 K as calculated in classical constant-*NVT* empirical potential simulations for a variety of supercell sizes.

Supercell	N (Å^2)	D (Å^2)	r_{cut} (Å)
2×2×2	0.00580(1)	0.01317(1)	4.82
3×3×3	0.00673(1)	0.01417(1)	7.23
4×4×4	0.00746(1)	0.01510(1)	9.64
6×6×6	0.00789(1)	0.01559(1)	14.46

super-cells are required to fully converge the displacement parameters. Figure 3 shows the N–N radial distribution functions with 2×2×2 and 4×4×4 supercells. At 77 K, the two cell sizes give identical short-range behavior, while the longer-range peaks are slightly broader in the 4×4×4 simulation; this effect is somewhat more apparent at 180 K. These results demonstrate that system-size effects, probably arising either as a result of the imposition of constraints on the momentum of the center-of-mass of the system or due to the artificial dynamic correlations introduced in small supercells, can significantly influence calculated properties relating to thermal motion.

Unfortunately, while it is evident that there is some finite-size effect in these empirical force-field simulations it is not so clear how this transfers to DFT simulations. An important parameter in empirical simulations is the cut-off distance, r_{cut}, after which intermolecular dispersion interactions are neglected; this distance must be less than half of the simulation box length. Thus, in empirical MD simulations a large cell can be required for an atom to have enough dispersive and repulsive interactions so that it truly behaves as if it was in the solid state. In a DFT simulation the periodicity of the wave functions ensures that this problem does not arise, although artificial dynamic correlations may still persist between atoms in neighboring cells. In any event, the

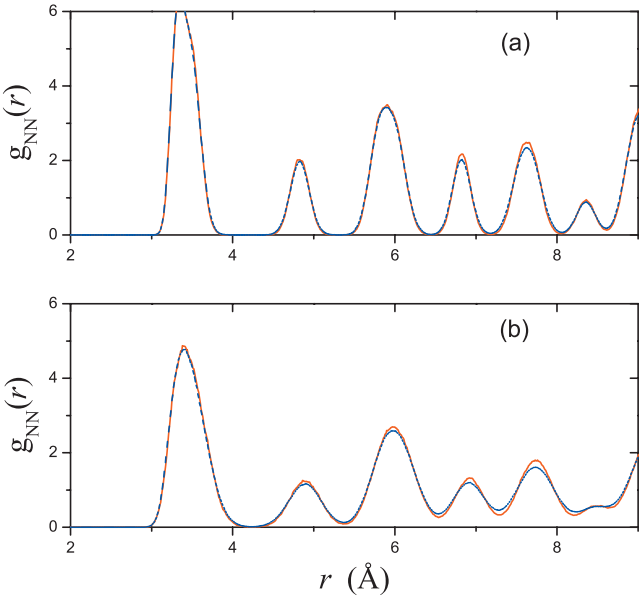

FIG. 3. Classical N–N radial pair distribution functions at (a) 77 K and (b) 180 K. The solid red line represents the results of a simulation for a 2×2×2 supercell; the blue dashed line a 4×4×4 cell.

TABLE IV. Isotropic displacement parameters (U_{eq}) of the N and D atoms for three different unit cell sizes. Values were calculated in classical constant-*NVT* empirical potential MD simulations of a 4×4×4 supercell.

a (Å)	N (Å^2)	D (Å^2)	$\langle P \rangle$ (GPa)
4.75	0.00624(1)	0.01363(1)	0.63
4.82	0.00741(1)	0.01519(1)	0.05
4.89	0.00891(1)	0.01699(1)	−0.35

change in the isotropic displacement parameters upon moving from a 2×2×2 supercell to a 6×6×6 in the empirical MD simulations cannot account for the relatively large discrepancies between the DFT simulation results and the experimental results.

2. Simulation pressure

A further possible source of error in the DFT simulations is the use of an optimized lattice parameter, rather than a finite-temperature value. In the case of the 77 K DFT simulations the use of an optimized lattice parameter results in an average pressure of 0.1 GPa during the course of the simulation. It seems unlikely that this would affect the potential energy surface (and hence thermal motion) substantially as the structure of phase-I ammonia is stable up to 1.4 GPa Ref. 11 and the N–H vibrational frequencies change by less than 5 cm^{-1} over this pressure range.[36]

However, to test the influence of the unit cell parameter on the thermal motion, we performed classical empirical MD simulations at 77 K with a 4×4×4 super-cell of ND_3 using three different cell vectors: 4.82 Å (corresponding to the unit cell at ambient pressure in a classical MD simulation), 4.75, and 4.89 Å. The results of these simulations are given in Table IV. The pressure has been calculated using the standard virial estimator.[29] The ambient pressure of 0.05 GPa is quite large but illustrates the problem of converging the cell vector with respect to pressure. We find that decreasing the unit cell length by 0.07 Å results in a substantial increase in pressure. However, the large increase in pressure from 0 GPa to 0.63 GPa only leads to changes in the order of 15% in the thermal parameters. As the pressure in the 77 K DFT simulations was much smaller (0.1 GPa) it is therefore unlikely that our choice of unit cell parameters in the DFT simulations has a large effect on the calculated thermal motions.

3. Nuclear quantum effects

As discussed in Sec. III A, one of the most likely faults with the DFT simulations is the assumption that the nuclei behave classically. To investigate the influence of nuclear quantum effects, PIMD simulations with the empirical HC force field were performed at 77 and 180 K and compared with equivalent classical MD simulations. In both cases, simulations were performed using a 4×4×4 supercell.

The results of this comparison are given in Table V, where we consider the influence of temperature and the number of ring-polymer beads (imaginary-time slices) used in the PIMD simulations. At the lower temperature of 77 K, nuclear quantum effects play a significant role in the thermal motion.

TABLE V. Isotropic displacement parameters (U_{eq}) of the N and D atoms in ND_3 from $4\times4\times4$ simulations at 77 and 180 K, as determined in classical ($P=1$) and PIMD ($P=32,64$) simulations with different numbers of ring-polymer beads (imaginary-time slices), P.

P	T (K)	N (Å^2)	D (Å^2)
1	77	0.00741(1)	0.01519(1)
32	77	0.00979(1)	0.02649(1)
64	77	0.00966(1)	0.02668(1)
1	180	0.02196(1)	0.04565(1)
32	180	0.02295(1)	0.05356(1)

Comparing the results of the $P=64$ ring-polymer bead calculation to the classical result ($P=1$), we find that quantum fluctuations increase the isotropic displacement parameter for N by 30% and for D by about 75%; this difference is not surprising given the light mass of deuterium. Finally, we note that a comparison of a $P=64$ ring-polymer bead simulation and a $P=32$ simulation at 77 K demonstrates that our results are converged with respect to P.

If we assume that the magnitude of nuclear quantum effects is independent of the chosen potential energy function, we can use the results of these empirical PIMD simulations to correct the results of classical DFT simulations for the influence of quantum fluctuations. At 77 K, this correction gives U_{eq} values of 0.0136 and 0.0243 Å for the N and D atoms, respectively. These values compare well with the values of Leclercq *et al.*, 0.0144(3) and 0.0222(4) Å.

At the higher temperature of 180 K, the N atom and D atom isotropic displacement parameters are increased relative to the classical values by 4% and 17%, respectively; as expected, the contribution of quantum nuclear effects is much smaller than that determined at 77 K. We note that the classical empirical MD displacement parameters at 180 K are much larger than those determined in classical DFT simulations, whereas at 77 K the classical empirical MD displacement parameters were smaller than the DFT values. Inspection of the simulation trajectories shows that there is complete rotation of the ND_3 molecules about the molecular and crystallographic C_3 axis in the empirical MD simulations; this behavior is not seen in the high-temperature DFT MD simulation.

The experimental melting point of phase-I ammonia is 195.3 K,[37] which is not far from the higher simulation temperature of 180 K. Thus, it is quite likely that our empirical potential simulations or DFT simulations are not correctly modeling thermal motion near the melting transition. It is well-known that DFT simulations of hydrogen-bonded systems, such as liquid water,[38] can result in a range of calculated physical properties, depending upon the simulation details and chosen functionals. We might expect an empirical potential primarily tested in the liquid phase to model the onset of the phase transition better, but this is by no means guaranteed. We have not calculated the melting point of phase-I ammonia using the HC force field; determining melting points by simulation is by no means trivial and is beyond the scope of this present study. Given these observations, the development and validation of a new interaction potential by crystalline ammonia would be beneficial, particularly in light of the importance of solid ammonia in extraterrestrial atmospheres.

IV. CONCLUSION

In this work, we have investigated thermal motion in phase-I deuteroammonia at 77 and 180 K using a combination of classical MD simulations with DFT and quantum PIMD simulations with an empirical force field.

At both temperatures, our classical DFT simulations predicted significantly less thermal motion than originally determined in the experimental refinement of Hewat and Riekel. However, our DFT simulations were in very good agreement with a more recent refinement of the same experimental data performed by Leclercq *et al.*, particularly at higher temperature. Given that this later refinement employed an analysis technique which more accurately accounted for librational motion, we suggest that the earlier refinement of Hewat and Riekel contains some errors in the extracted displacement parameters.

At the lower temperature of 77 K, our classical DFT simulations show a much larger level of disagreement with the recent Leclercq refinement. We find that at least some of this discrepancy can be accounted for by nuclear quantum effects. By determining the typical thermal motion arising due to nuclear quantum effects in a PIMD simulation using an empirical potential, we have corrected the results of our classical DFT simulations. The isotropic displacement parameters determined after applying these corrections are then in good agreement with the latest experimental refinement. We have also investigated the influence of system size and unit cell parameters on the simulation of ammonia's thermal motion; such effects were not able to account for the discrepancies between our classical DFT simulations and the experimental results, whereas nuclear quantum effects were found to play a more significant role. Overall, our results demonstrate how a simulation approach combining classical DFT simulations, classical empirical force-field simulations and quantum PIMD simulations can provide insight into thermal motion in crystalline structures, as well as allow cross-validation of simulation and experimental results.

A new neutron diffraction study of ammonia would be useful to remove doubts surrounding the Hewat and Riekel data set, especially as the solid-state N–H/D bond length appears to be shorter than the gas-phase value recently determined using high-level theory and experiment.[34] While the reanalysis of Leclercq *et al.* clearly addresses many of the issues with the orginal powder diffraction refinement the limited Q-range of the data set means that the rerefined solid-state bond length has a large uncertainty ($\sim$0.005 Å). This large uncertainty means that no significance can be attached to the observation of a shorter solid-state N–D/H bond length. A new experiment would also be useful to clarify how well DFT describes crystalline ammonia and for assessing the validity of different empirical interaction potentials.

ACKNOWLEDGMENTS

The empirical potential simulations were performed using the resources of the EaStCHEM Research Computing Facility (http://www.eastchem.ac.uk/rcf). This facility is partially supported by the eDIKT initiative (http://www.edikt.org.uk). The DFT-MD simulation made use of the Edinburgh Parallel Computing Centre (http://www.epcc.ed.ac.uk). We thank Professor David Manolopoulos for comments on a draft of this manuscript. A.M.R. acknowledges the School of Chemistry, Edinburgh for funding a studentship, C.A.M. acknowledges the Royal Society for the award of a University Research Fellowship, and S.H. acknowledges the U.S. Office of Naval Research for funding under contract No. N000140510460.

[1] A. W. Hewat and C. Riekel, Acta Crystallogr. A **35**, 569 (1979).
[2] G. Sill, U. Fink, and J. R. Ferraro, J. Opt, Soc. Am. **70**, 724 (1980).
[3] P. G. J. Irwin, Surv. Geophys. **20**, 505 (1999).
[4] J. S. Kargel, Icarus **100**, 556 (1992).
[5] J. W. Reed and P. M. Harris, J. Chem. Phys. **35**, 1730 (1961).
[6] R. Boese, N. Neiderprüm, D. Bläser, A. Maulitz, M. Yu. Antipin, and P. R. Mallinson, J. Phys. Chem. B **101**, 5794 (1997).
[7] P. Damay, F. Leclercq, and P. Chieux, Phys. Rev. B **41**, 9676 (1990).
[8] O. S. Binbrek and A. Anderson, Chem. Phys. Lett. **15**, 421 (1972).
[9] J. S. Holt, D. Sadoskas, and C. J. Pursell, J. Chem. Phys. **120**, 7153 (2004).
[10] M. Powell, G. Dolling, G. S. Pawley, and J. W. Leech, Can. J. Phys. **58**, 1703 (1980).
[11] M. M. Siddick, G. J. Ackland, and C. A. Morrison, J. Chem. Phys. **125**, 064707 (2006).
[12] A. M. Reilly, D. S. Middlemiss, M. M. Siddick, D. A. Wann, G. J. Ackland, C. C. Wilson, D. W. H. Rankin, and C. A. Morrison, J. Phys. Chem. A **112**, 1322 (2008).
[13] A. Hinchliffe, D. G. Bounds, M. L. Klein, I. R. McDonald, and R. Righini, J. Chem. Phys. **74**, 1211 (1981).
[14] V. Schomaker and K. N. Trueblood, Acta Crystallogr., Sect. B: Struct. Crystallogr. Cryst. Chem. **24**, 63 (1968).
[15] D. W. J. Cruickshank, Acta Crystallogr. **9**, 757 (1956).
[16] F. Leclercq, P. Damay, and M. Foukani, J. Chem. Phys. **102**, 4400 (1995).
[17] A. M. Reilly, D. A. Wann, C. A. Morrison, and D. W. H. Rankin, Chem. Phys. Lett. **448**, 61 (2007).
[18] J. P. Perdew, K. Burke, and M. Ernzerhof, Phys. Rev. Lett. **77**, 3865 (1996).
[19] J. P. Perdew, J. A. Chevary, S. H. Vosko, K. A. Jackson, M. R. Perderson, D. J. Singh, and C. Fiolhais, Phys. Rev. B **46**, 6671 (1992).
[20] J. P. Perdew, J. A. Chevary, S. H. Vosko, K. A. Jackson, M. R. Perderson, D. J. Singh, and C. Fiolhais, Phys. Rev. B **48**, 4978 (1993).
[21] M. Parrinello and A. Rahman, J. Chem. Phys. **80**, 860 (1984).
[22] R. P. Feynman and A. R. Hibbs, *Quantum Mechanics and Path Integrals* (McGraw-Hill, New York, 1965).
[23] CPMD, Version 3.13.2, IBM Corp. 1990–2008, MPI für Festkörperforschung, Stuttgart, 1997–2001, 2008.
[24] N. Troullier and J. L. Martins, Phys. Rev. B **43**, 1993 (1991).
[25] H. J. Monkhorst and J. D. Pack, Phys. Rev. B **13**, 5188 (1976).
[26] R. Car and M. Parrinello, Phys. Rev. Lett. **55**, 2471 (1985).
[27] D. J. Tobias, G. J. Martyna, and M. L. Klein, J. Phys. Chem. **97**, 12959 (1993).
[28] M. Diraison, G. J. Martyna, and M. E. Tuckerman, J. Chem. Phys. **111**, 1096 (1999).
[29] M. P. Allen and D. J. Tildesley, *Computer Simulation of Liquids* (Oxford University, New York, 1989).
[30] H. C. Andersen, J. Chem. Phys. **72**, 2384 (1980).
[31] H. Flyvbjerg and H. G. Petersen, J. Chem. Phys. **91**, 461 (1989).
[32] The 77 K DFT-MD values reported here are slightly different from those previously given in Ref. 17. A mistake in the orginal analysis resulted in an overestimation of sampling uncertainties. The correct values are provided here.
[33] J. Haestier, M. Sadki, A. L. Thompson, and D. Watkin, J. Appl. Crystallogr. **41**, 531 (2008).
[34] C. Puzzarini, Theor. Chem. Acc. **120**, 325 (2008).
[35] G. Martyna and M. E. Tuckerman, J. Chem. Phys. **110**, 2810 (1999).
[36] C. L. Nye and F. D. Medina, Phys. Rev. B **32**, 2510 (1985).
[37] *CRC Handbook of Chemistry and Physics*, 89th ed., edited by D. R. Lide (CRC Press/Taylor and Francis, Boca Raton, FL, 2009).
[38] M. Sprik, J. Phys.: Condens. Matter **8**, 9405 (1996).